Effect of the Compatibility on the Morphology and Properties of Acrylonitrile–Butadiene Rubber/ Polypropylene Thermoplastic Vulcanizates

Ming Tian,[1,2] Jibin Han,[1] Hanguang Wu,[1] Hongchi Tian,[1] Qingyan She,[1] Wenquan Chen,[1] Liqun Zhang[1,2]

[1]*Key Laboratory of Carbon Fiber and Functional Polymers, Ministry of Education, Beijing University of Chemical Technology, Beijing 100029, China*
[2]*Key Laboratory of Beijing City on Preparation and Processing of Novel Polymer Materials, Beijing University of Chemical Technology, Beijing 100029, China*

Received 11 April 2011; accepted 8 July 2011
DOI 10.1002/app.35222
Published online 25 October 2011 in Wiley Online Library (wileyonlinelibrary.com).

ABSTRACT: In this study, the morphologies of three types of acrylonitrile–butadiene rubber (NBR)/polypropylene (PP) thermoplastic vulcanizates (TPVs) (with an NBR/PP blend ratio of 70/30) were compared. The TPVs were (1) an ultrafine fully vulcanized acrylonitrile–butadiene rubber (UFNBR)/PP TPV made by the mechanical blending of UFNBR with PP, (2) a dynamically vulcanized NBR/PP TPV without the compatibilization of maleic anhydride grafted polypropylene (MP) and amine-terminated butadiene–acrylonitrile copolymer (ATBN), and (3) a dynamically vulcanized NBR/PP TPVs with the compatibilization of MP and ATBN. The influence of the compatibility therein on the size of the dispersed vulcanized NBR particles and the crystallization behavior of the PP in the TPVs and the resultant properties are also discussed. As indicated by Fourier transform infrared spectroscopy, scanning electron microscopy, differential scanning calorimetry, polarizing microscopy, dynamic mechanical thermal analysis, and rheological and mechanical testing, the compatibility was significantly improved by the reactive compatibilization of MP and ATBN, which led to a uniform and fine morphology. The compatibilization increased the crystallization rate and reduced the size of the spherulites of PP. On the other hand, it was found that the dispersed vulcanized NBR particles lowered the degree of crystallinity. The better the compatibility of the blend was, the lower the degree of crystallinity and the storage modulus were, but the higher the loss factor and the processing viscosity were. All TPVs showed almost the same oil resistance, but the TPV prepared with reactive compatibilization had the best mechanical properties. J Appl Polym Sci 124: 1999–2006, 2012

Key words: compatibility; morphology; poly(propylene) (PP)

INTRODUCTION

Thermoplastic vulcanizates (TPVs) prepared with the dynamic vulcanization method possess the same excellent elasticity as rubber and the same processability as thermoplastics. Also, they can easily be recycled or reused to save petroleum resources and reduce environmental pollution.[1–6] TPVs are attracting much more attention than before and have become a research focus in the field of polymer materials.

Dynamic vulcanization is recognized as an important method for producing thermoplastic elastomers with a variety of properties and functions. TPVs are made from existing rubbers and thermoplastics without the need to synthesize new polymers. Some typical TPVs that have been commercialized include ethylene–propylene–diene rubber/polypropylene (PP), acrylonitrile–butadiene rubber (NBR)/PP, and silicon rubber/polyamide blends.[2–6] TPVs can also be produced by the direct blending of preprepared ultrafine fully vulcanized rubber particles in the size of 50–150 nm with thermoplastics.[7–9]

The compatibility of blends significantly influences the morphology of TPVs and thus influences their mechanical properties, rheological properties, and crystallization behavior. Compatibility between rubber and plastics is essential because blends with poor compatibility are unstable, and thus, the similar phases of the blends easily self-aggregate.[10] Coran and Patel[5,11,12] found that NBR/PP TPVs with excellent mechanical properties could be prepared with the compatibilization of maleic anhydride grafted

Correspondence to: L. Zhang (zhanglq@mail.buct.edu.cn).
Contract grant sponsor: National Basic Research Program (973 Program) of China; contract grant numbers: 2011CB606000 and 2011CB606003.
Contract grant sponsor: Chang-Jiang Scholar Program of the Ministry of Education of China; contract grant number: IRT0807.

polypropylene (MP) and amine-terminated butadiene–acrylonitrile copolymer (ATBN). Soares and coworkers[13,14] successfully prepared NBR/PP TPVs by using MP as a compatibilizer and dicumyl peroxide in combination with *N,N′-m*-phenylene bismaleimide (BMI) as cocuring agents. Corley and Radusch[15] studied the compatibilization of each of the reactant pairs, MP and ATBN, maleic anhydride grafted ethylene–propylene–diene rubber and ATBN, and maleic anhydride grafted styrene–ethylene–butadiene–styrene and ATBN on NBR/PP TPVs. It was found that the reactant pair of MP and ATBN was the best compatibilizer of the three. Zhang et al.[16] found that NBR/PP TPVs with excellent mechanical properties could be prepared by using glycidyl methacrylate grafted PP/diethylenetriamine as compatibilizers and *t*-butyl phenolic resin as the curing agent.

In this study, the morphologies of three types of NBR/PP TPVs (with a constant mass ratio of NBR to PP of 70/30) were investigated in detail. The TPVs were ultrafine fully vulcanized acrylonitrile–butadiene rubber (UFNBR) particle/PP TPVs made by the mechanical blending of preprepared UFNBR particles with PP, dynamically vulcanized NBR/PP TPV, and dynamically vulcanized NBR/ATBN/PP/MP TPV with the compatibilization of MP and ATBN. The influence of the compatibilization on the size of the NBR particles, crystallization behavior of PP in the TPVs, and mechanical properties, rheological properties, and oil resistance of the TPVs are also discussed.

EXPERIMENTAL

Materials

PP (HP500D) was supplied by Basell Co., Ltd. (Bangkok, Thailand). NBR (230 s) was bought from Nippon Zeon Co., Ltd. (Tokyo, Japan). UFNBR (Narpow VP-401) particles were obtained from Beijing Research Institute of Chemical Industry of China Petroleum and Chemical Corp. (Beijing, China). ATBN (HYCAR ATBN 1300 × 16) was provided by Noveon Co., Ltd. (Hongkong, China) MP (CMG0101) was obtained from Sunrise Co., Ltd. (Shanghai, China). Pentaerythritol tetrakis[β-(3,5-di-*tert*-butyl-4-hydroxyphenyl) propionate] (antioxidant 1010), $SnCl_2{\cdot}2H_2O$, and dimethylol phenolic resin SP1045 were commercially available.

Sample preparation

Preparation of UFNBR/PP TPV

The UFNBR/PP TPV was prepared by the direct blending of UFNBR with PP at a mass ratio of 70/30 in a Haake mixer (Type PolyLabA, Thermo Fisher Scientific Co., Ltd. (Karlsruhe, Germany)). The mixing temperature was 180°C, and the rotational rate was 80 rpm. The mixing time was 10 min.

Preparation of NBR/PP TPV

NBR/PP TPV was prepared by dynamic vulcanization. NBR and PP were first mixed for 3 min at a mass ratio of 70/30 in the same Haake mixer. The mixing temperature was 180°C, and the rotational rate was 80 rpm. The vulcanizing agent (dimethylol phenolic resin SP1045, 5 phr) and the accelerator ($SnCl_2{\cdot}2H_2O$, 0.5 phr) were then added, and mixing was continued for another 7 min. The total mixing time was 10 min.

Preparation of NBR/ATBN/PP/MP TPV

NBR/ATBN/PP/MP TPV was prepared by dynamic vulcanization. NBR (65 phr), ATBN (5 phr), PP (27 phr), and MP (3 phr) were first mixed for 3 min in the same Haake mixer. The mixing temperature was 180°C, and the rotational rate was 80 rpm. The vulcanizing agent (SP1045, 5 phr) and the accelerator ($SnCl_2{\cdot}2H_2O$, 0.5 phr) were then added, and mixing was continued for another 7 min. The total mixing time was 10 min.

The compositions of the three types of TPVs and the NBR vulcanizate are shown in Table I.

Fourier transform infrared (FTIR) measurements

The possible reaction between the maleic anhydride groups of MP and the amine groups of ATBN was measured with an EQUINOX55FT-IR, Bruker FTIR spectrometer Bruker Co., Ltd. (Billerica, United States). MP and ATBN were blended at a mass ratio of 5 : 3 in the Haake mixer for 5 min, and the mixing temperature was set at 180°C. The blend of MP and ATBN used for the measurements was pressed into thin films at 200°C.

Morphological analysis

The samples for morphological studies were prepared by cryogenic fracturing in liquid nitrogen and etched by hot xylene to remove the PP phase. The original and etched fracture surfaces were sputter-coated with gold. The photographs were taken on a Cambridge S-250-III scanning electron microscope (SEM), Cambridge Scientific Instruments Co., Ltd., (Cambridge, Britain).

Differential scanning calorimetry (DSC) analysis

The crystallization and melting behavior of the samples were analyzed by a Mettler-Toledo Stare DSC1, Mettler-Toledo Co., Ltd., (Zurich, Swizerland) instrument in a nitrogen atmosphere. The instrument was calibrated with indium before testing.

For crystallization analysis, the sample was heated to 200°C rapidly, maintained at this temperature for 5 min to eliminate any previous thermal history, and

TABLE I
Compositions of Three Types of TPVs and the NBR Vulcanizate

Ingredient	UFNBR/ PP TPV	NBR/ PP TPV	NBR/ATBN/ PP/MP TPV	NBR
PP	30	30	27	—
NBR	—	70	65	100
UFNBR	70	—	—	—
ATBN	—	—	5	—
MP	—	—	3	—
$SnCl_2{\cdot}2H_2O$	—	0.5	0.5	0.5
SP1045	—	5	5	5
1010	0.5	0.5	0.5	—

then cooled at two different rates (5 and 10°C/min) to observe the nonisothermal crystallization behavior. After crystallization, the sample was heated to 200°C at a rate of 10°C/min, and the melting behavior of the sample was observed.

Polarizing microscopy (PLM) analysis

The crystallization morphologies of PP and the TPVs were studied with an SM-LUX, Leitz Co., (Wetzlar, Germany) polarizing microscope. A test sample was prepared as follows. A small amount of PP or TPV was placed on a glass slide and heated to and maintained for 5 min at 200°C to remove any prior thermal history. The sample was pressed into a thin film between two glass slides and quickly transferred to a vacuum oven for isothermal crystallization. The morphology of the crystals was observed, and photographs were taken.

Dynamic mechanical thermal testing

The dynamic mechanical properties of the samples were measured in tension mode with a VA3000 instrument (DMTA, 01dB-Metravib company, Lyons, France) at a frequency of 1 Hz. Samples 15 × 6 × 2 mm^3 were used for the study. The temperature range used was from −75 to +150°C, and the heating rate was 5°C/min.

Rheological behavior

The melt rheological behavior of the samples was analyzed in a rubber process analyzer (RPA 2000, Alpha Technologies company, Ohio, United States). All of the samples were directly loaded between the dies maintained at 190°C, and the tests were carried out in strain sweep modes. The strain amplitude sweep was performed from 1 to 1200% at a constant frequency of 0.1 Hz.

Mechanical properties

The Shore A hardness of the sample was measured according to ASTM D 2240. The tensile properties were measured according to ASTM D 412 on a CMT 4104 testing machine, MTS Systems Corporation, (Shenzhen, China) with dumbbell-shaped samples at a crosshead speed of 500 mm/min. The tear strength was measured according to ASTM D 624 with unnicked 90°-angle test pieces. The crosshead speed was the same as that used for tensile testing.

The compression set of the cylindrical specimen with a diameter of 29.0 mm and a height of 12.5 mm was measured according to ASTM D 624. We performed the tests by pressing the specimen to 10% of its original height, and the specimen was kept at 100°C for 22 h. After the fastening clips were removed, the final thickness of the specimen was measured after 0.5 h of exposure at room temperature.

Oil-resistance analysis

Oil resistance was measured according to ASTM D 471. The samples were immersed in ASTM #3 oil at 125°C for 72 h. The samples were then removed from the oil and wiped with filter paper to remove the excess oil from the surface, and their weights were measured in air and water.

RESULTS AND DISCUSSION

Reaction between MP and ATBN

The maleic anhydride in MP could react with the terminal amine in ATBN at the NBR/PP interface, and this led to the formation of a block copolymer, which reduced the interfacial tension and improved the compatibility between NBR and PP. The reaction is illustrated as follows:

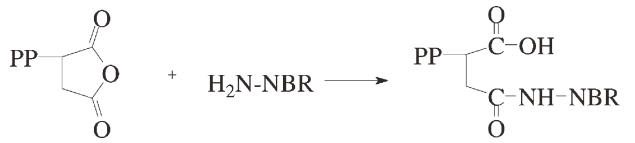

As shown in Figure 1, the peaks at 1784 and 1864 cm^{-1}, which were attributed to the stretching

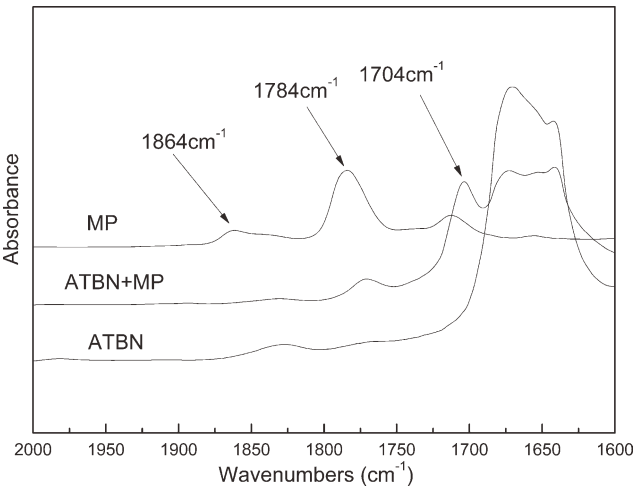

Figure 1 FTIR spectra of MP, ATBN, and their reaction product.

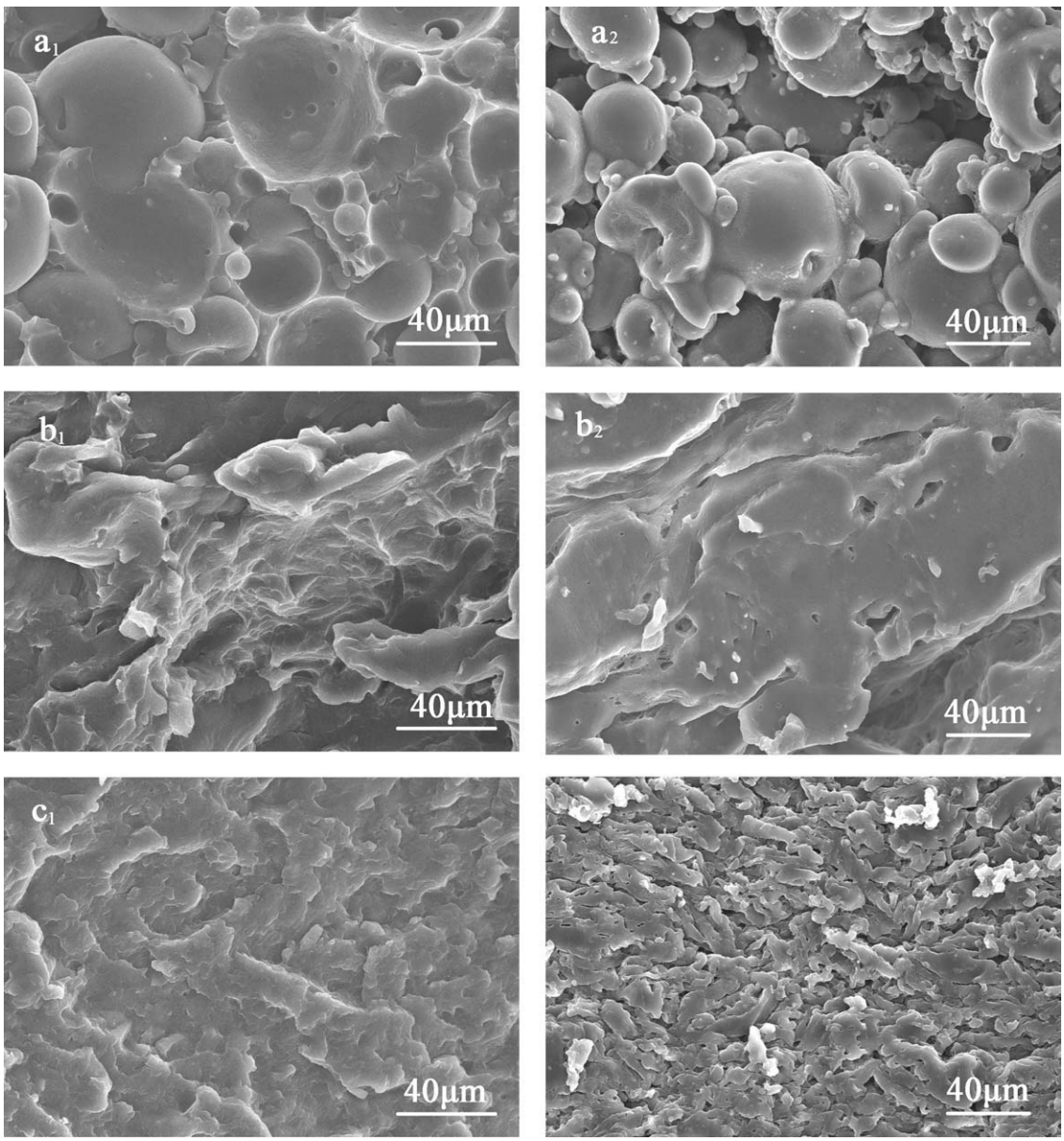

Figure 2 Scanning electron micrographs of three types of NBR/PP TPVs: (a) UFNBR/PP TPV, (b) NBR/PP TPV, and (c) NBR/ATBN/PP/MP TPV.

vibrations of the carbonyl groups of the maleic anhydride in MP, disappeared or weakened in the FTIR spectra of the block copolymer of MP and ATBN. The new vibration peak was observed at 1704 cm^{-1}, which was attributed to the stretching vibrations of maleimide of the block copolymer. These features suggested that the maleic anhydride in MP reacted with the terminal amine in ATBN to form a block copolymer.

Morphology of the NBR/PP TPVs

Figure 2 shows the scanning electron micrographs of the three types of NBR/PP TPVs. Figure 2(a1,b1,c1) shows the original fracture surfaces, and Figure 2(a2,b2, c2) shows the etched fracture surfaces. As shown in Figure 2(a1, a2), the shape of the UFNBR domains in the PP matrix was spherical originally, the fractured interface was smooth, and some UFNBR particles were protuberant; this suggested a poor interface between PP and UFNBR. During dynamic vulcanization, cured NBR was broken by shear stresses into irregular particles. For the dynamically vulcanized NBR/PP TPV, as shown in Figure 2(b1,b2), the dispersed NBR particles were so large that their ductile fracture led to extremely rough sections. With the addition of the compatibilizer, the NBR particles became smaller and were more uniformly dispersed, as shown in Figure 2(c1,c2); this led to relatively flat and ductile sections.

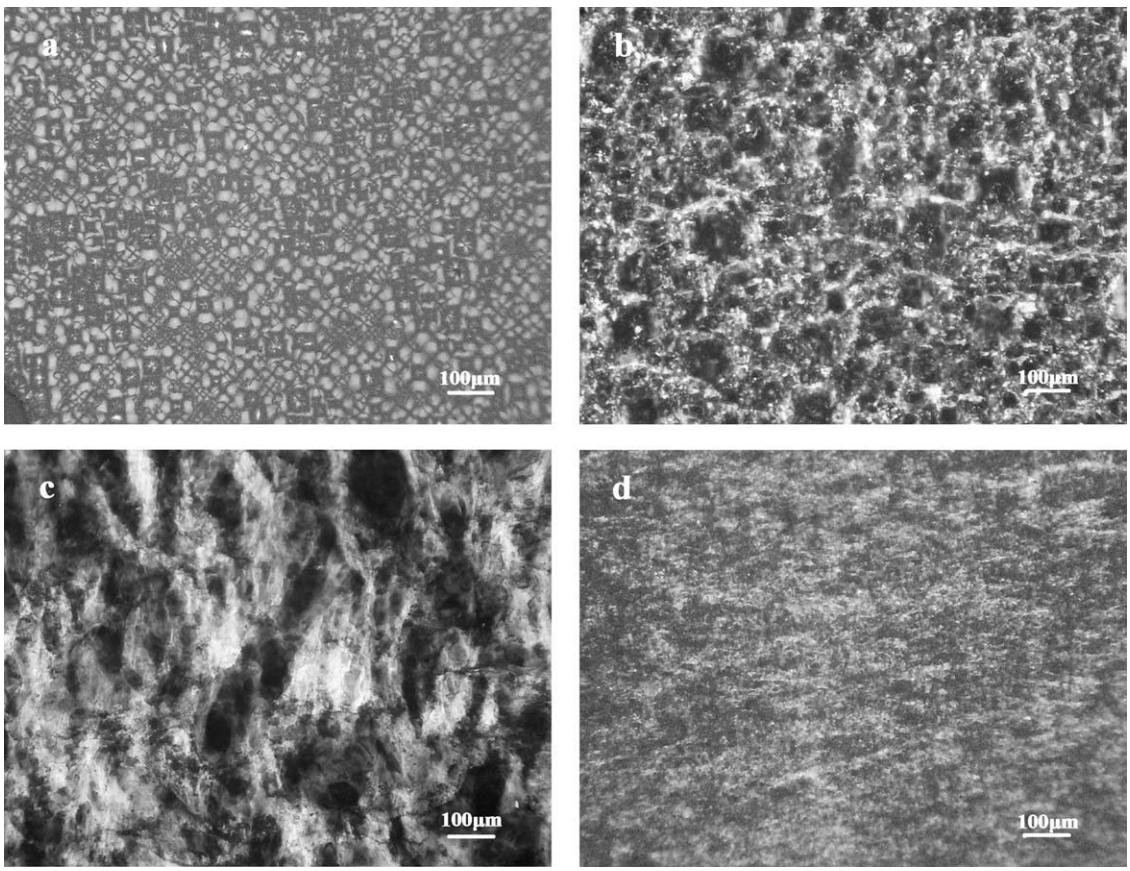

Figure 3 PLM images of PP and three types of NBR/PP TPVs: (a) PP, (b) UFNBR/PP TPV, (c) NBR/PP TPV, and (d) NBR/ATBN/PP/MP TPV.

PLM study

The mechanical properties of polymers are closely related to the crystallization behavior and ultimate spherulite structure. PP generally forms large and perfect spherulites upon homogeneous nucleation and small and imperfect spherulites upon heterogeneous nucleation.[7,17–19] The morphology of PP spherulites can be observed through PLM. Figure 3 shows the PLM images of PP and the three types of TPVs. The dark areas in the micrographs represent the dispersed domain of vulcanized NBR and the amorphous phase of PP, and the white areas show the crystalline phase of PP. There were a lot of full and uniformly dispersed Maltese crosses for pure PP, an indication of perfect crystallization [Fig. 3(a)]. The growth of PP spherulites in all of the NBR/PP TPVs was retarded because of the separation of vulcanized NBR particles, so more small bright dots were observed instead of the Maltese crosses. On the other hand, the distribution of these small PP spherulites could indicate the dispersion of NBR particles. For NBR/ATBN/PP/MP TPV, the addition of the compatibilizer increased the compatibility between NBR and PP, so NBR formed smaller and more uniform particles than NBR/PP TPV in PP by dynamic vulcanization. The smaller and more uniform particles induced uniform heterogeneous nucleation and resulted in more and smaller polymer crystals, as indicated in Figure 3(d). The compatibilizer was absent in dynamically vulcanized NBR/PP TPV and UFNBR/PP TPV, so the NBR particles were not dispersed uniformly [Fig. 3(b,c)].

DSC analysis

Table II shows the results obtained from DSC analysis. The *half-crystallization time* ($t_{1/2}$), which is defined as the time at a relative degree of crystallinity (X_c) of 50%, could be directly obtained from the DSC curves. The smaller the value of $t_{1/2}$ was, the higher the crystallization rate. X_c could be calculated as follows:[20]

$$X_c = \Delta H/\Delta H_m \times 100$$

where ΔH is the normalized enthalpy of fusion per gram of sample measured at the melting temperature (T_m) and ΔH_m is the enthalpy of fusion of the perfectly crystalline PP (100% X_c). The value of ΔH_m was 209 J/g.

TABLE II
$t_{1/2}$, T_m, and X_c Values of PP, NBR, and the Three Types of NBR/PP TPVs

Sample	$t_{1/2}$ (s)		T_m (°C)		X_c (%)	
	a	b	a	b	a	b
PP	322.8	158.0	166.8	166.5	42.5	41.6
UFNBR/PP TPV	133.4	85.9	165.4	165.2	40.2	38.7
NBR/PP TPV	165.2	93.6	164.8	164.5	38.7	38.4
NBR/PP/ATBN/MP TPV	91.0	40.0	164.6	164.1	38.6	37.5

a: cooling rate = 5°C/min; b: cooling rate = 10°C/min.

Table II shows that the three types of TPVs had much lower $t_{1/2}$ values than PP did. The lower $t_{1/2}$ values were attributed to the nucleating effect of the NBR particles on PP crystallization. In addition, the crystallinity of PP was a little higher than any of the three types of TPVs; this indicated that the addition of NBR had an adverse effect on the crystallinity of PP. Of the three types of TPVs, NBR/ATBN/PP/MP TPV had the lowest crystallinity, probably because the presence of the block copolymer generated by MP and ATBN at the NBR/PP interface hindered the motion and folding of the PP molecular chains. On the other hand, the smaller and more uniformly dispersed NBR particles in NBR/ATBN/PP/MP TPV might have retarded the formation of full and large PP spherulites because the PP molecular chains were separated by the NBR particles. The lower X_c led to a lower value of T_m.

Dynamic mechanical thermal analysis

Figure 4(a) shows the temperature dependence of the storage modulus for PP, NBR, and the three types of TPVs. It can be seen that the storage modulus of PP was the highest and that of NBR was the lowest. The addition of NBR to PP lowered the modulus of PP. This phenomenon was more obvious with the better compatibility between the two phases, when the disturbance of the rubber molecular chains on the PP chains was stronger. Because PP is a highly crystalline polymer, its storage modulus was still high, even at the glass-transition temperature.

Figure 4(b) shows the temperature dependence of damping (tan δ) for PP, NBR, and the three types of TPVs. The peak of the tan δ curve corresponded to the glass-transition temperature. It could be seen that NBR showed the highest tan δ peak, whereas PP showed the lowest peak. The tan δ peaks of all of the TPVs were higher than that of pure PP, and the peaks increased with increasing amount of NBR. The better the compatibility between NBR and PP was, the higher the effect of NBR was. We concluded that the viscoelasticity of the TPVs was partly determined by the NBR dispersed phase, which was related to the compatibility of NBR and PP.

Rheological properties

Figure 5 presents the strain dependence of the storage modulus for PP and the three types of NBR/PP TPVs. In filled elastomer systems, with increasing strain amplitude at a constant frequency, the dynamic storage modulus decreases. This phenomenon is called the *Payne effect*.[21] The attenuation of storage modulus with strain is mainly attributed to the breakdown of the filler network. A rapid attenuation of storage modulus indicates a strong filler

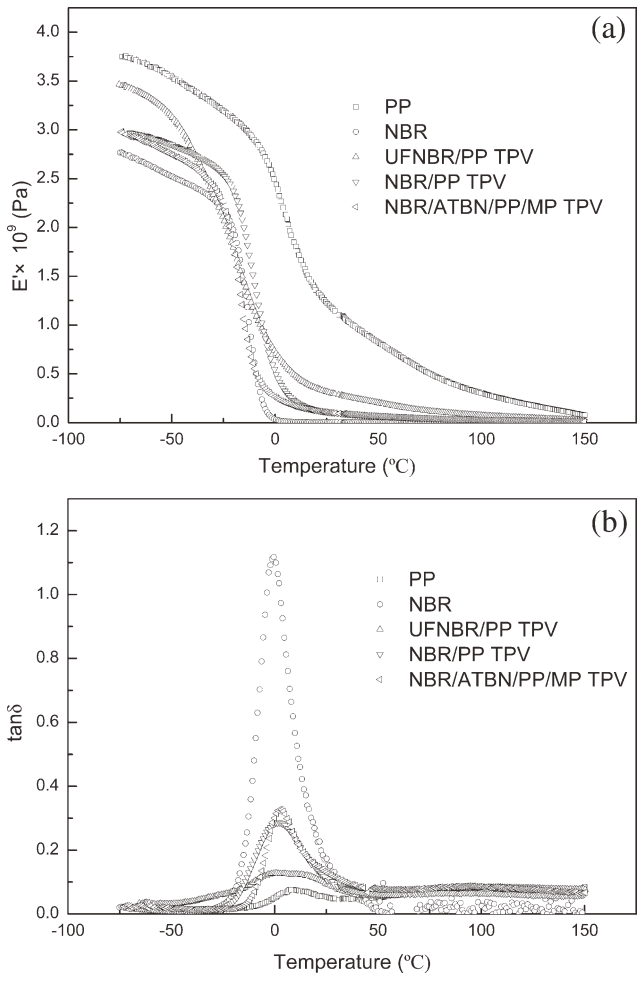

Figure 4 Temperature dependence of the (a) storage modulus (E') and (b) tan δ for PP, NBR, and three types of TPVs.

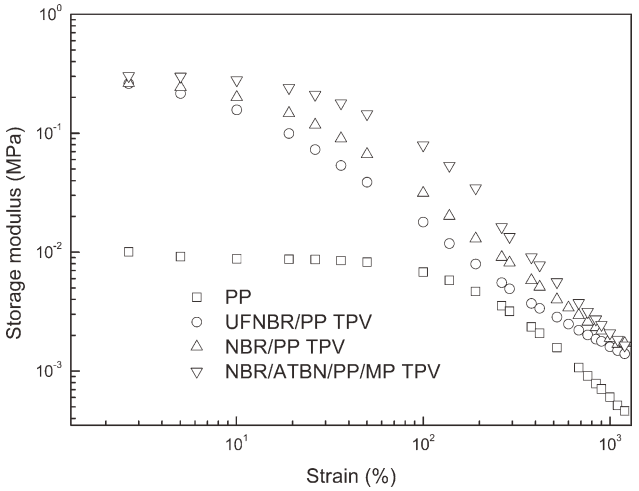

Figure 5 Storage modulus as a function of the strain amplitude for PP, NBR, and three types of NBR/PP TPVs at 190°C.

network. In TPVs, a decrease in the dynamic storage modulus corresponds to the agglomeration of crosslinked rubber particles dispersed in the continuous plastic matrix.[22–24] As shown in Figure 5, the three types of TPVs exhibited much higher initial storage moduli (at very low strains) than pure PP as a result of the filler network created by the vulcanized NBR particles. The higher initial storage modulus also indicated a higher processing viscosity. All three types of TPVs had almost the same initial storage modulus, but NBR/PP/ATBN/MP TPV showed the slowest attenuation of storage modulus; this suggested that the filler network in NBR/PP/ATBN/MP TPV was the weakest. The vulcanized NBR particles were well encapsulated by PP molecular chains because of the strong interactions (good compatibility) between the NBR particles and PP chains, so that the NBR particles could not be in direct contact with each other; thus, the filler network in NBR/PP/ATBN/MP TPV was the weakest.

Mechanical properties and oil-resistance behavior of the TPVs

Table III shows that the TPVs prepared with the reactive compatibilization possessed the lowest hardness and significantly improved tensile strength, tear strength, and ultimate elongation values. Compression set is one of the most important properties characterizing the elasticity of TPVs. Of the three types of TPVs, NBR/ATBN/PP/MP TPV had the lowest compression set. The three types of TPVs had almost the same oil resistance; however, the TPVs prepared by dynamic vulcanization showed a somewhat worse oil resistance compared to the other two types. The lower oil resistance of NBR/ATBN/PP/MP TPV could have been due to its lower X_c relative to UFNBR/PP TPV. In general, the higher X_c is, the better the oil resistance will be.

CONCLUSIONS

The compatibility of the NBR/PP blends had significant effects on the dispersed NBR particles size and the crystallization behavior of the PP matrix. The better the compatibility was, the smaller the size and the more uniform the distribution of the NBR particles were. With the resulting heterogeneous nucleation, PP showed a higher crystallization rate, higher crystallization temperature, and smaller spherulites. The dispersed vulcanized NBR particles lowered the degree of crystallization of PP. The better the compatibility of the blend was, the lower X_c and storage modulus were, but the higher the loss factor and processing viscosity were. The compatibility was significantly improved by the reactive compatibilization of MP and ATBN, which led to better mechanical properties but about the same oil resistance as the other two types of TPVs without compatibilization.

TABLE III
Mechanical Properties and Oil Resistance of the Three Types of NBR/PP TPVs

Sample	UFNBR/ PP TPV	NBR/ PP TPV	NBR/ATBN/PP/MP TPV		
			a	b	c
Hardness, Shore A	97	95	94	93	91
Tensile strength (MPa)	9.5	13.2	19.3	23.5	20.6
Ultimate elongation (%)	123	168	257	310	262
100% Modulus (MPa)	7.5	8.4	9.1	10.7	10.3
Tear strength (kN/m)	48.7	52.6	68.4	70.6	65.8
Compression set (%)	75	62	58	53	56
Oil resistance, weight change (%)	15.3	16.1	16.6	16.8	17.1

a: MP = 1 phr and ATBN = 5 phr; b: MP = 3 phr and ATBN = 5 phr; c: MP = 8 phr and ATBN = 5 phr.

References

1. Gessler, M. U.S. Pat. 3,037,954 (1962).
2. Fisher, K. U.S. Pat. 3,758,643 (1973).
3. Coran, A. Y.; Patel, R. U.S. Pat. 4,104,210 (1978).
4. Coran, A. Y.; Patel, R. Rubber Chem Technol 1980, 53, 141.
5. Coran, A. Y.; Patel, R. Rubber Chem Technol 1983, 56, 1045.
6. Coran, A. Y.; Patel, R.; Williams, D. Rubber Chem Technol 1982, 55, 116.
7. Xu, X. D.; Qiao, J. L.; Yin, J. H.; Gao, Y.; Zhang, X. H.; Ding, Y. T.; Liu, Y. Q.; Xin, Z. R.; Gao, J. M.; Huang, F.; Song, Z. H. J Polym Sci Part B: Polym Phys 2004, 42, 1042.
8. Huang, F.; Liu, Y. Q.; Zhang, X. H.; Wei, G. S.; Gao, J. M.; Song, Z. H.; Zhang, M. L.; Qiao, J. L. Macromol Rapid Commun 2002, 23, 786.
9. Zhang, M. L.; Liu, Y. Q.; Zhang, X. H.; Gao, J. M.; Huang, F.; Song, Z. H.; Wei, G. S.; Qioa, J. L. Polymer 2002, 43, 5133.
10. Okada, O.; Keskkula, H.; Paul, D. R. Polymer 2000, 41, 8061.
11. Coran, A. Y.; Patel, R. U.S. Pat. 4,299,931 (1981).
12. Coran, A. Y.; Patel, R. U.S. Pat. 4,409,365 (1983).
13. Soares, B. G.; Almeida, M. S.; Deepa, M. V. J Appl Polym Sci 2006, 102, 4672.
14. Soares, B. G.; Oliveira, M. D.; Meireles, D.; Sirqueira, A. S.; Mauler, R. S. J Appl Polym Sci 2008, 110, 3566.
15. Corley, B. E.; Radusch, H. J. J Macromol Sci Phys 1998, 37, 265.
16. Zhang, X. F.; Huang, H.; Zhang, Y. X. J Appl Polym Sci 2002, 85, 2862.
17. Huang, H.; Liu, X.; Ikehara, T.; Nishi, T. J Appl Polym Sci 2003, 90, 824.
18. Cui, L. M.; Wang, S. F.; Zhang, Y.; Zhang, Y. X. J Appl Polym Sci 2007, 105, 379.
19. Jiang, X. L.; Zhang, Y.; Zhang, Y. X. J Polym Sci Part B: Polym Phys 2004, 42, 1181.
20. Greco, R.; Mancarella, C.; Martuscelli, E.; Ragosta, G.; Yin, J. Polymer 1987, 28, 1929.
21. Payne, A. R. Reinforcement of Elastomers; Interscience: New York, 1965; Chapter 3.
22. Marinvic, T.; Susteric, Z.; Dimitrievski, I.; Veksli, Z. Kautsch Gummi Kunstst 1998, 51, 189.
23. Babu, R. R.; Singha, N. K.; Naskar. J Appl Polym Sci 2010, 117, 1578.
24. Saleesung, T.; Saeoui, P.; Sirisinha, C. Polym Test. 2010, 29, 977.